Research Paper

Distinct fiber-specific white matter reductions pattern in early- and late-onset Alzheimer's disease

Xiao Luo[1,*], Shuyue Wang[1,*], Yeerfan Jiaerken[1], Kaicheng Li[1], Qingze Zeng[1], Ruiting Zhang[1], Chao Wang[1], Xiaopei Xu[1], Dan Wu[2], Peiyu Huang[1,#], Minming Zhang[1,#], Alzheimer's Disease Neuroimaging Initiative (ADNI)

[1]Department of Radiology, The 2nd Affiliated Hospital of Zhejiang University School of Medicine, Hangzhou, China
[2]Key Laboratory for Biomedical Engineering of Ministry of Education, College of Biomedical Engineering and Instrument Science, Zhejiang University, Hangzhou, China
*Equal contribution
#Joint senior author

Correspondence to: Minming Zhang; **email:** zhangminming@zju.edu.cn
Keywords: fixel-based analysis, early-onset Alzheimer's disease, diffusion magnetic resonance imaging, white matter, amyloid deposition
Received: October 7, 2020 **Accepted:** February 8, 2021 **Published:** April 30, 2021

Copyright: © 2021 Luo et al. This is an open access article distributed under the terms of the Creative Commons Attribution License (CC BY 3.0), which permits unrestricted use, distribution, and reproduction in any medium, provided the original author and source are credited.

ABSTRACT

Background: The underlying white matter impairment in patients with early and late-onset Alzheimer's disease (EOAD and LOAD) is still unclear, and this might due to the complex AD pathology.
Methods: We included 31 EOAD, 45 LOAD, and 64 younger, 46 elder controls in our study to undergo MRI examinations. Fiber density (FD) and fiber bundle cross-section (FC) were measured using fixel-based analysis based on diffusion weighted images. On whole brain and tract-based level, we compared these parameters among different groups (p<0.05, FWE corrected). Moreover, we verified our results in another independent dataset using the same analyses.
Results: Compared to young healthy controls, EOAD had significantly lower FD in the splenium of corpus callosum, limbic tracts, cingulum bundles, and posterior thalamic radiation, and higher FC in the splenium of corpus callosum, dorsal cingulum and posterior thalamic radiation. On the other hand, LOAD had lower FD and FC as well. Importantly, a similar pattern was found in the independent validation dataset. Among all groups, both the FD and FC were associated with cognitive function. Furthermore, FD of fornix column and body, and FC of ventral cingulum were associated with composite amyloid and tau level (r=-0.34 and -0.53, p<0.001) respectively.
Conclusions: EOAD and LOAD were characterized by distinct white matter impairment patterns, which may be attributable to their different neuropathologies.

INTRODUCTION

Alzheimer's disease (AD) can be commonly categorized as either early onset (EOAD) or late onset (LOAD) based on an age cutoff of 65 years [1]. Comparing to LOAD, EOAD has relatively more aggressive disease course and shorter survival time [2], and their clinical symptoms are usually more occult despite occurring at a younger age. In addition to memory deficits, EOAD has lower performance in attention, visuospatial skills, and executive functions than LOAD [3, 4]. Although both EOAD and LOAD share the same neuropathological hallmarks (i.e., amyloid plaques and neurofibrillary tangles), distinct

distribution patterns were found by previous post-mortem and *in vivo* imaging studies [5, 6]. Surprisingly, EOAD patients have a higher burden of amyloid deposition and neurofibrillary tangles than LOAD in frontal and parietal lobes [7–9], which is incompatible with their aging process.

Although AD is famous for cortical neurodegenerative pathology, recent studies using conventional diffusion tensor imaging (DTI) technique have also implicated white matter (WM) abnormalities in the risk and progression of AD [10–13]. Canu et al. also found that LOAD had altered fractional anisotropy (FA) and mean diffusivity (MD) in the posterior cingulum, corpus callosum, and temporal lobes, while EOAD had more diffuse WM abnormalities [14]. Although past studies have shed light on the investigation of WM degeneration in EOAD, the interpretation of diffusion imaging results was still greatly affected by the complexity of fiber bundle geometry considering crossing fibers account for up to 90% of whole brain WM voxels. Unfortunately, conventional diffusion tensor model cannot represent multiple, independent intra-voxel orientations thus fails to fit complex crossing fibers [15]. For instance, if a voxel contains multiple crossing fibers with different WM component, conventional DTI model can only describe the local FA, MD measures, each while microstructural (or macrostructural) information which is specific to the fiber orientation cannot be quantified. Since AD shows different forms of WM degeneration such as fiber atrophy (macroscopic level) and demyelination (microscopic level), the inability of DTI to capture different WM alterations complicates the interpretation of WM abnormalities thus further limits the use of this conventional method in neurodegenerative disease like AD. In short, the voxel-averaged metrics derived from DTI is neither fiber-specific nor easily interpretable.

To fill in the blanks, a novel diffusion model named fixel-based analysis (FBA) has been proposed in recent years [16]. The term "fixel" represents all the different fiber bundles with different orientations within a "voxel". Each fixel carriers microstructural or macrostructural information, which is specific to the fiber orientation. The commonly investigated metrics of fixel-based analysis are fiber density (FD) and fiber cross-section (FC), reflecting the fibers density within a fiber bundle and macro-structural property of fiber bundles, respectively [17]. Additionally, fiber density and fiber cross-section (FDC) incorporates both the microscopic and macroscopic degenerative processes [18, 19]. A recent work showed that FBA could accurately reflect the microstructural differences between AD and healthy elderly, and more importantly, these results are biologically interpretable [18]. To date, this advanced method has been successfully applied in various neurodegenerative diseases, including AD and Parkinson disease [17, 18, 20].

In this cross-sectional study, FBA was applied to two independent datasets of EOAD and LOAD. We aimed to 1) investigate the white matter impairments in EOAD and LOAD; 2) establish the relation between FBA metrics like FD, FC, FDC, and other AD related measures including cognitive function and AD neuropathologies. Considering the distinct clinical and neuropathological features of EOAD and LOAD [6–9], we hypothesized that LOAD has a preferential loss in fiber bundles connecting to the medial temporal regions, while EOAD has more widespread impairments in WM tracts.

RESULTS

Demographics

AD patients and control subjects did not differ significantly in age, sex and education. For each dataset, there is no significant difference between EOAD and LOAD, or YHC and OHC in general cognitive score ($p > 0.05$). Furthermore, there is no interaction relationship between the onset age (<65 or ≥ 65 years) and the disease status (whether healthy or not) ($p > 0.05$). Notably, patients from the ADNI dataset had milder disease severity and higher education level than those patients from the ZJU dataset (Supplementary Material 1).

Whole-brain fixel-based analysis results

ZJU database

EOAD had a diffuse decrease of FD in SCC, column and body of fornix, left fornix-HP, bilateral dorsal/ventral cingulum, and PTR; additionally, EOAD had a decrease of FC in SCC, bilateral dorsal cingulum, and PTR. Regarding the composite index (FDC), EOAD had a decrease of FDC in the SCC, left fornix-hippocampus, bilateral dorsal/ventral cingulum, and PTR as compared to YHC. We also found that LOAD had a decrease of FD in the bilateral dorsal/ventral cingulum and left ILF/IFOF and a decrease of FC in the SCC, bilateral dorsal/ventral cingulum, PTR, and ILF/IFOF as compared to OHC. Moreover, LOAD had a decreased of FDC in the SCC, bilateral dorsal/ventral cingulum, ILF/IFOF, and PTR (Figure 1).

ADNI database

EOAD had significantly lower FD in the CC, column and body of fornix, and left ventral cingulum as compared to YHC, while there is no significant difference in FC was found between EOAD and YHC.

EOAD had lower FDC in the left ventral cingulum. On the other hand, LOAD had lower FD in the SCC, column and body of fornix, right fornix-hippocampus, and left ventral cingulum as compared to OHC. In addition, LOAD had lower FC in the column and body of fornix, left dorsal cingulum, and lower FDC in the SCC and left dorsal/ventral cingulum (Figure 1).

Repeatability test of whole-brain fixel-based analysis results

To eliminate the potential statistical bias due to differences in patient demographics from two independent datasets, we matched two datasets based on their age, sex and basic demographics. After conducting the same analysis on this combined dataset, the results we yielded were with similar patterns despite of the fact

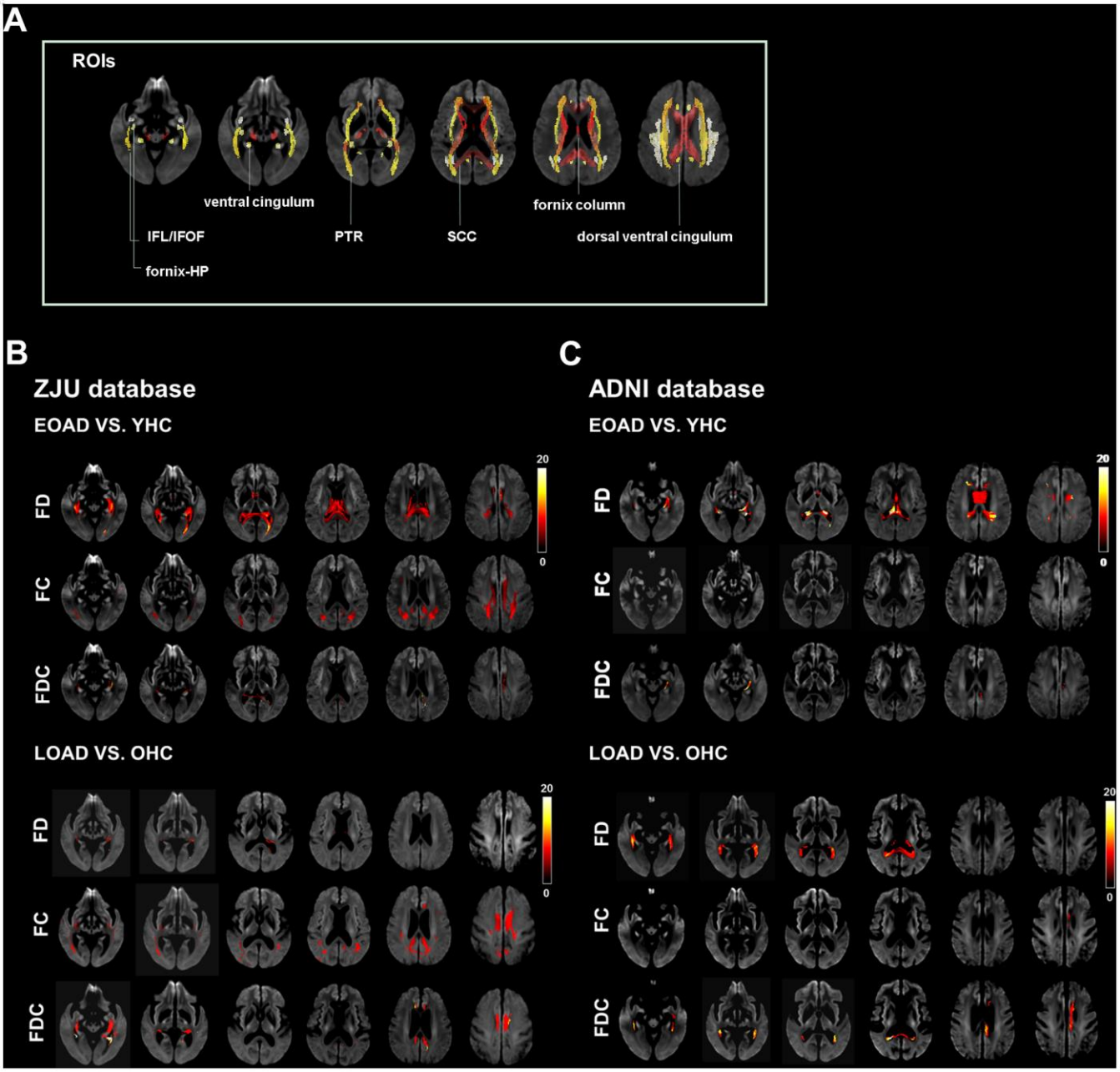

Figure 1. The location reference and fiber tract-specific reduction in EOAD/LOAD versus controls from whole-brain fixel-based analysis. (**A**) illustrates the location reference. (**B**) and (**C**) Represent results from ZJU and ADNI databases, respectively. We color-coded the significant streamlines by the effect size expressed as a percentage relative to the control groups. Abbreviations: ZJU, Zhejiang University; FD, fiber density; FC, fiber bundle cross-section; FDC, fiber density and bundle cross-section.

that the altered areas we detected were smaller in combined dataset compared to previous mentioned results (Supplementary Material 2).

Besides, AD is a multifactorial disease with multiple contributors to its pathophysiology, including cerebral small vascular disease (CSVD) [21]. Recent work suggested that the effects of CSVD on WM integrity should also be accounted for [22]. After adjusting for WMH, we repeated the same analyses in both ZJU and ADNI datasets and the results we yielded remained mostly unchanged despite of a lower but statistically sound significance level (Supplementary Material 3). In general, our results were consistent with recent findings and suggested that to some extent, WMH did contribute to part of the microstructural alterations in AD patients.

Tract level analysis

ZJU database

EOAD had lower mean FD in the SCC, fornix column and body, bilateral dorsal/ventral cingulum, right PTR, left fornix-hippocampus, as well as lower mean FC in the SCC, bilateral dorsal cingulum and PTR compared to YHC. Moreover, EOAD had lower mean FDC in the SCC, bilateral cingulum bundles and PTR, and left fornix-hippocampus compared to YHC. On the other hand, LOAD had lower mean FD in the right dorsal cingulum, bilateral ventral cingulum, ILF/IFOF, as well as lower mean FC in the SCC, bilateral ILF/IFOF and PTR compared to OHC. In addition, LOAD demonstrated decreased mean FDC in the SCC, bilateral cingulum bundles, ILF/IFOF, and PTR when compared to OHC (Figure 2).

ADNI database

EOAD had lower mean FD in the column and body of fornix and left ventral cingulum. However, there is no difference in mean FC and FDC between EOAD and YHC. On the other hand, comparing to YHC, LOAD had significantly decreased mean FD in the column and body of fornix, bilateral ventral cingulum, as well as decreased mean FC in the column and body of fornix. LOAD also had decreased FDC in left cingulum HP.

Relationship between fixel-based metrics and cognition/neuropathologies

Among all groups (EOAD, YHC, LOAD, and OHC), we correlated both the mean FD and FC with the cognitive assessment (Figure 3). Here we only displayed the significant associations between FBA metrics (i.e., FD and FC) and total MMSE/CDR. With the ADNI dataset, we also correlated the FBA metrics with PET-derived AD neuropathological markers. Correlation results in subgroup level were shown in Supplementary Material 4.

ZJU database

We found that the MMSE was associated with the FD in the SCC ($r = 0.33$, $P < 0.001$), bilateral dorsal cingulum ($r = 0.40/0.38$, $P < 0.001$), left ventral cingulum ($r = 0.48$, $P < 0.001$), bilateral ILF/IFOF ($r = 0.23/0.25$, $P < 0.001$), while the total CDR was associated with the FD in the SCC ($r = -0.31$, $P < 0.001$), bilateral dorsal cingulum ($r = -0.28/-0.26$, $P < 0.001$), left ventral cingulum ($r = -0.42$, $P < 0.001$). On the other hand, we found that the MMSE was correlated with the FC in the SCC ($r = -0.35$, $P < 0.001$), bilateral dorsal cingulum ($r = 0.26/0.33$, respectively, $P < 0.001$), ILF/IFOF ($r = 0.28/0.25$, $P < 0.001$), and PTR ($r = 0.39/0.43$, respectively, $P < 0.001$), while the total CDR was correlated with the FC in the SCC ($r = -0.29$, $P < 0.001$), left dorsal cingulum ($r = -0.28$, $P < 0.001$), and bilateral PTR ($r = -0.32/-0.35$, $P < 0.001$, Figure 3).

ADNI database

We found that the MMSE was correlated with the FD in the SCC ($r = 0.33$, $P < 0.001$), bilateral dorsal cingulum ($r = 0.40/0.38$, respectively, $P < 0.001$), left ventral cingulum ($r = 0.48$), and bilateral ILF/IFOF ($r = 0.23/0.25$, $P < 0.001$), while the total CDR was correlated with the FD in SCC ($r = -0.31$, $P < 0.001$), bilateral dorsal cingulum ($r = -0.28/-0.26$, $P < 0.001$), and left ventral cingulum ($r = 0.42$, $P < 0.001$). On the other hand, the MMSE was correlated with the FC in the SCC ($r = 0.35$, $P < 0.001$), bilateral dorsal cingulum ($r = 0.26/0.33$, $P < 0.001$), ILF/IFOF ($r = 0.28/0.25$, $P < 0.001$), PTR ($r = 0.39/0.43$, $P < 0.001$); while the total CDR was correlated with the FC in the SCC ($r = -0.29$, $P < 0.001$), left dorsal cingulum ($r = -0.28$, $P < 0.001$), and bilateral PTR ($r = -0.32/-0.35$, respectively, $P < 0.001$, Figure 3).

Associations between FBA metrics and PET data

Among all groups, the FD of column and body of fornix was correlated with the composite amyloid deposition SUVR ($r = -0.34$), while the FC of right ventral cingulum was correlated with the mean tau retention of Braak I-II ROI, including the bilateral entorhinal and hippocampus ($r = -0.53$). Figure 4 illustrates the hypothetical model of white matter pathological processes in EOAD and LOAD.

DISCUSSION

In current study, we used FBA to study the WM impairments in EOAD and LOAD and further validated our results on another entirely independent dataset. The major findings include: (i) LOAD had severer but more spatially confined WM impairments along the limbic-related tracts, while EOAD had more widely distributed WM impairments involving the limbic-related tracts, the column and body of fornix, left fornix-HP, SCC,

and PTR even after correcting for WMH burden; (ii) the WM impairment we found in EOAD was majorly characterized by decreased FD rather than FC in both datasets; (iii) both FD and FC were associated with the cognitive function and greater disease burden. More importantly, based on the ADNI database, the decreased FD and FC were associated with increased SUVR of amyloid and tau, respectively. Conclusively, our results

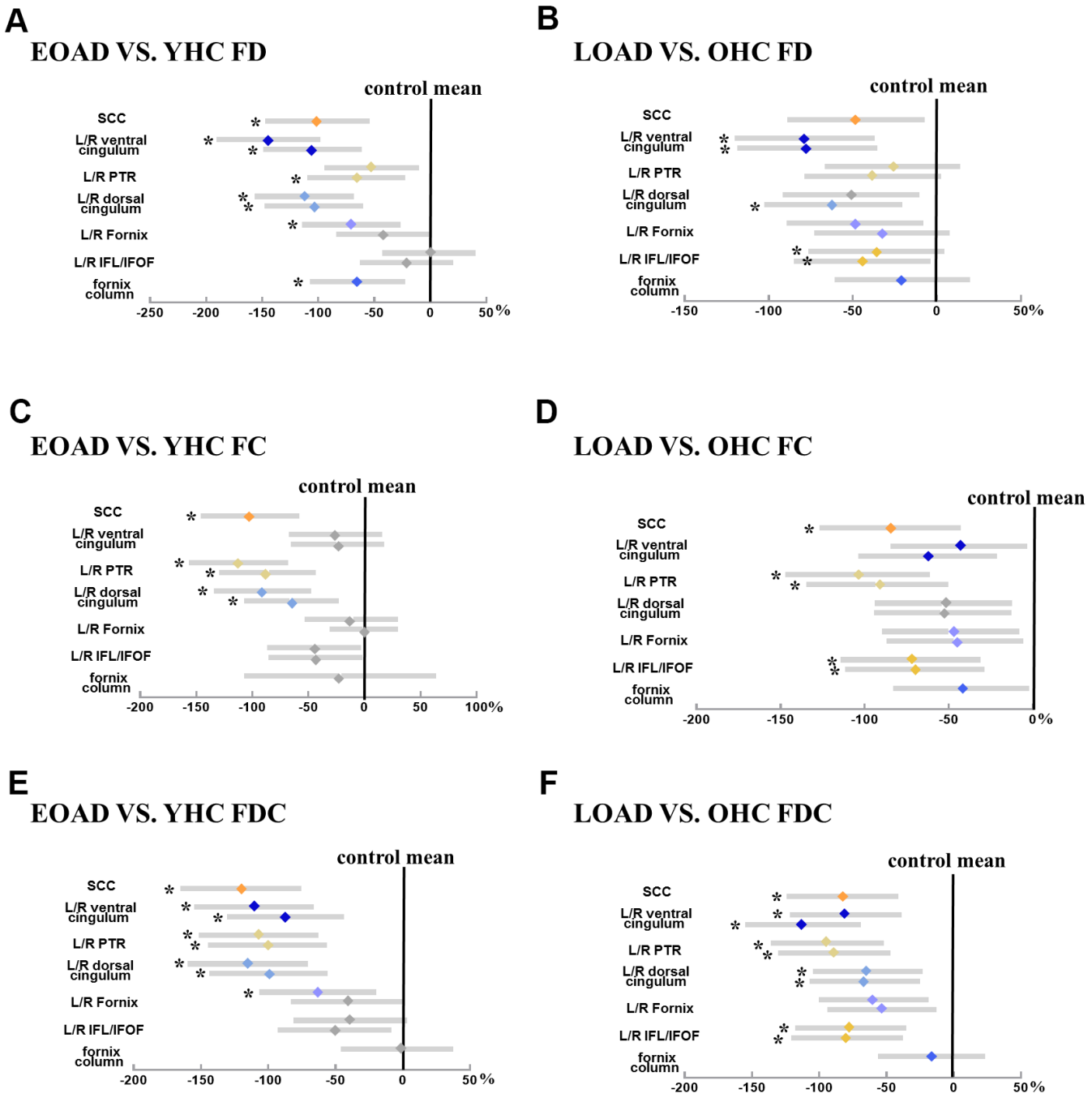

Figure 2. The group difference (patient VS. control) in mean FD, FC, and FDC based on the ZJU database. (**A**, **C**, **E**) Represents the mean FD, FC, and FDC (diamond) and 95% CI (bars) within tracts of interest are displayed for early-onset Alzheimer's disease groups, respectively; (**B**, **D**, **F**) represents the mean FD, FC, and FDC (diamond) and 95% CI (bars) within tracts of interest are displayed for late-onset Alzheimer's disease groups, respectively. The more the color bar shifted to the left, representing more significant difference from healthy controls. Notably, significant tracts (Bonferroni-corrected P-value < 0.05, controlling for age and sex) are marked with star symbols. Abbreviation: SCC, splenium of the corpus callosum; ILF/IFOF, inferior longitudinal fasciculus/inferior frontal-occipital fasciculus; PTR, posterior thalamic radiation; HP, hippocampus; FD, fiber density; FC, fiber bundle cross-section; FDC, fiber density and cross-section.

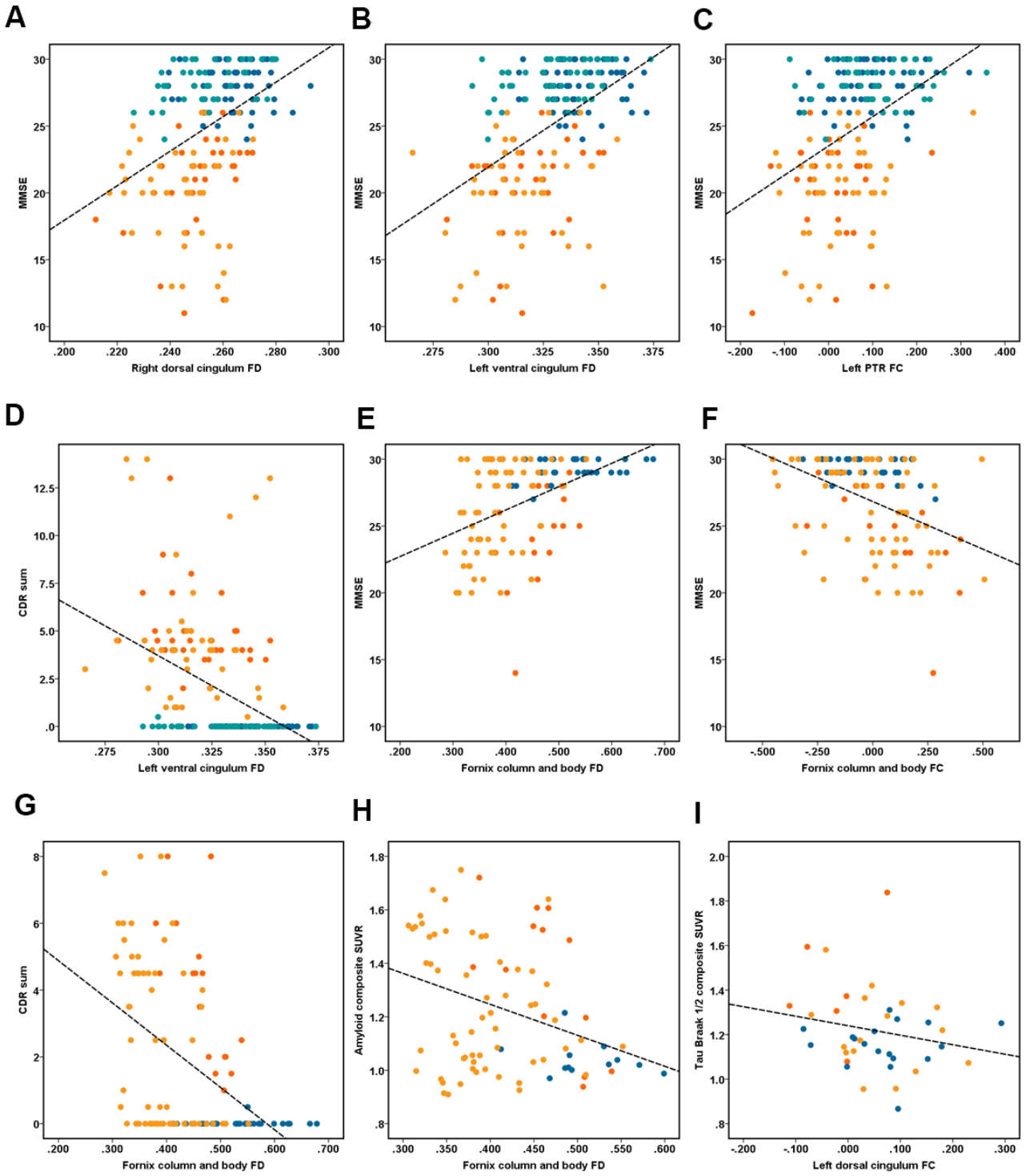

Figure 3. The association between fixel-based analysis metrics and clinical data. Correlation analyses of (**A**–**D**) performed in the ZJU database. (**A**) Right dorsal cingulum fiber density (FD) related with MMSE (r = 0.40, P < 0.001); (**B**) left ventral cingulum FD related with MMSE (r = 0.48, P < 0.001); (**C**) left PTR fiber bundle cross-section (FC) related with MMSE (r = 0.43, P < 0.001); (**D**) left ventral cingulum FD related with CDR sum (r = 0.42, P < 0.001). Correlation analyses of (**E**–**I**) performed in the ADNI database. (**E**) Fornix column and body FD related with MMSE (r = 0.45, P < 0.001); (**F**) fornix column and body FC related with MMSE (r = -0.42, P < 0.001); (**G**) fornix column and body FD related with CDR sum (r = -0.45, P < 0.001); (**H**) fornix column and body FD related with composite amyloid SUVR (r = -0.34, P < 0.001); (**I**) right ventral cingulum FC related with tau Braak I/II composite SUVR (r = -0.53, P < 0.001). Note: dot of red, orange, dark blue and light blue represent the early-onset Alzheimer's disease (EOAD), late-onset Alzheimer's disease (LOAD), young healthy controls (YHC), and old healthy controls (OHC).

suggested that EOAD and LOAD were featured by distinct WM impairment patterns thus may had different pathological mechanisms.

Distinct white matter impairment pattern in LOAD and EOAD patients

White matter impairments in LOAD were mostly located on the bilateral dorsal and ventral cingulum and ILF/IFOF in both datasets. Notably, white matter impairments of LOAD were more pronounced, though more spatially confined than EOAD. This result is consistent with past evidence that AD patients with a younger onset age have less pathology in the hippocampus but more extensive involvement of cortex [23]. Anatomically, the cingulum bundle connects the anterior medial prefrontal cortex, PCC, and medial temporal lobe, which are the hubs of default mode network (DMN) [24]. Besides, bilateral ILF/IFOF directly links the angular gyrus with the DMN [25]. Our results thus suggested that white matter tracts subserving the DMN are especially vulnerable to the effects of AD pathologies. Similarly, previous studies reported that LOAD patients were featured by restricted DMN disconnection [26–28].

On the contrary, EOAD patients exhibited additional white matter impairments in the column and body of fornix, left fornix-hippocampus, SCC, and PTR. Previous work also showed that EOAD patients have more widespread white matter microstructural impairment than LOAD [14, 29]. Our results are also supported by previous functional imaging evidence which showed that EOAD has various network dysfunction involving executive control, visuospatial, language, and memory-related networks [26–28]. Anatomically, the crura of fornix lies along the concavity of the hippocampus while the remainder is continued as the fimbria of hippocampus, which is prolonged into the uncus of the parahippocampal gyrus. SCC comprises the homotopic connections between the bilateral parietal and posterior cingulate cortices, which further form the executive-related network [30]. PTR connects the thalamus with the visual cortex, acting as the anatomical foundation of visuospatial and language function [31]. As we found the correlation between

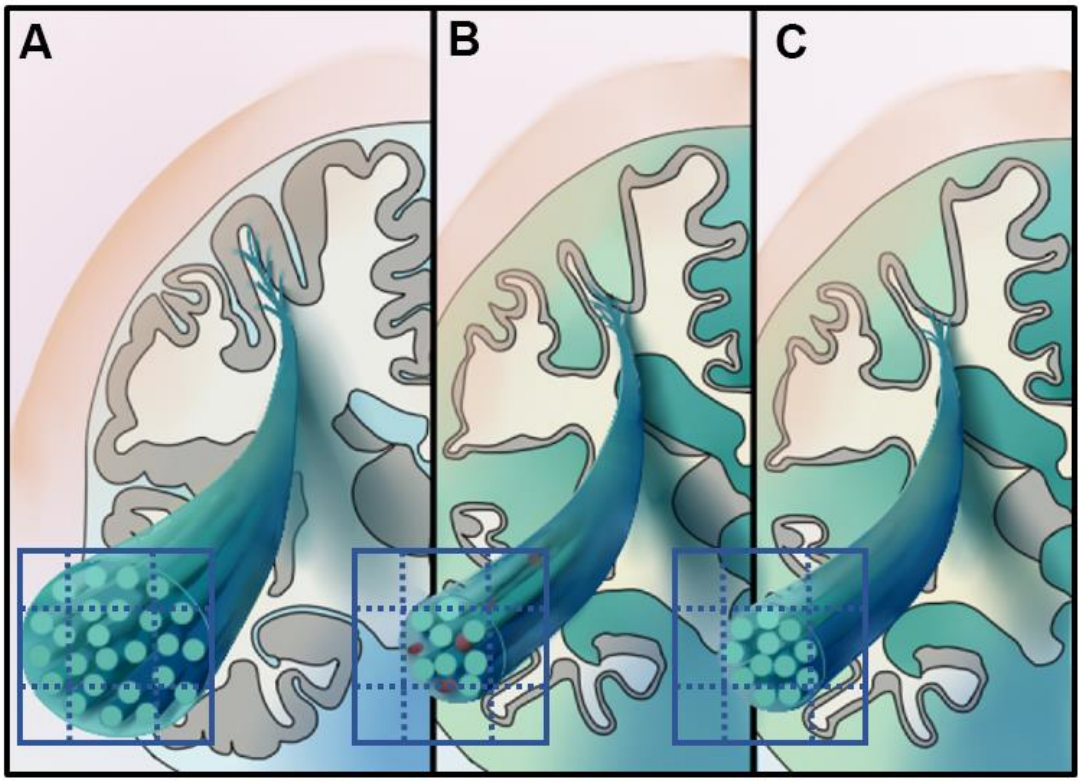

Figure 4. The hypothetical model of white matter pathological processes in early-onset Alzheimer's disease (EOAD) and late-onset Alzheimer's disease (LOAD). Specifically, 3D schematic represents a magnified fiber bundle, green tubule and grid on the cross-section represent the axons and imaging voxels, respectively. (**A**) Represents the healthy fiber bundle in the aging population. EOAD (**B**) might undergo white mater disruption involved both the microstructural and macrostructural level, while the macrostructural degeneration dominates white matter loss in LOAD (**C**).

fixel-based metrics and multi-domain cognitive functions, we thus speculated that the widespread white matter impairment we found accounts for the atypical symptoms in EOAD. Notably, after adjusting for WMH, our results show that the FBA results remained mostly unchanged in both ZJU and ADNI datasets, but the significance level somehow lowered. Our results suggested that WMH did contribute to part of the microstructural alterations in AD patients, which is in accordance with previous results [22]. Thus, it is necessary to take CSVD burden into account in future AD studies.

White matter damage of EOAD is featured by reduced FD

In the ZJU dataset, EOAD showed a decrease of both FD and FC, while in LOAD, the decrease of FC was more salient than FD. A decrease in FD usually represents lower volume fraction within a voxel, while a decrease in FC represents smaller cross-sectional area of fiber bundle's [16]. Thus, decrease in both FD and FC may represent two pathological processes. Reasonably, the white matter disruption in EOAD may result from the deposition of amyloid plaques and neurofibrillary tangles. In contrast, the white matter impairments in LOAD may largely result from neurofibrillary tangles. This hypothesis is supported by our correlation analysis which showed that FD and FC were associated with amyloid deposition and tau retention respectively. Our speculations are in line with previous neuropathological findings that EOAD had a higher burden of AD neuropathologies than LOAD. Additionally, in both EOAD and LOAD, we found that white matter tracts with lower FD (i.e., fornix-related tracts) were anatomically connected with the DMN, which is the region first affected by amyloid deposition pathologies. In contrast, tracts with lower FC are long projection fibers (e.g., PTR) from posterior cortices. This is consistent with past evidence that parietal white matter impairment in AD was caused more by neurofibrillary tangles than amyloid plaques [32].

Discrepancies between results from different datasets

Although most results we got from different datasets showed the same trend, there are still discrepancies even after matching the sample. In the ADNI dataset, the extent of FD and FC decrease is smaller than that from the ZJU dataset. Additionally, LOAD in ADNI demonstrated salient decrease in FD rather than FC, and vice versa for ZJU. Several reasons may contribute for this: first, the clinical symptoms for patients from the ADNI dataset are milder than that of the ZJU dataset. Accordingly, white matter tracts involved in the early AD continuum, such as cingulum bundles and fornix-related tracts, had impairments of similar extent across datasets [33]. Second, brain reserve may delay the neuropathological process [34]. Moreover, patients from ADNI dataset had a higher education level than that of the ZJU dataset.

There are also several limitations of our study. First, higher number of diffusion gradient directions and higher b-values might help to estimate intra-axonal volume fraction and multiple fiber orientations. Although the low b-value should not hold much influence over the FC, and FBA have previously been applied in neurological disorders using diffusion data with lower b-value [35–38] and lower gradient directions as well [17, 20]. Based on the results from test-retest analysis, we believe our study showed the possibility of applying advanced diffusion-based techniques to data acquired under clinical settings, which help probe different neurodegenerative processes. Second, FBA assumed that fiber orientation distribution function response is the same for all fiber populations. However, it is not only the intra-axonal space that will contribute to the diffusion signal, but the diffusivity or tortuosity of the extracellular space will also be confounded to the FOD amplitudes, which needs to be further validated. Third, based on the 2018 AD research framework, ATN biological diagnosis criteria is recommended to diagnose AD patients [39].

Conclusively, we investigated the white matter impairment pattern in EOAD and LOAD. We found that EOAD had more widespread white matter microstructural impairment than LOAD, which may contribute to their worse cognitive profiles. White matter microstructural and macrostructural impairments were respectively associated with amyloid and neurofibrillary tangles, implicating that the white matter of EOAD are more susceptible to amyloid deposition.

MATERIALS AND METHODS

Participant and neuropsychological assessment

Each participant underwent MRI scanning and neuropsychological evolutions, parts of them additionally underwent amyloid/tau PET scanning. In the database of Zhejiang University (ZJU), the diagnosis of probable AD was made by an experienced neurologist according to the NINCDS/ADRDA criteria. Additionally, the neurologist evaluated the neurological history, blood biochemical examination, and neuropsychological scales to exclude dementia from other causes. The age at disease onset was provided by the patient's family members or caregivers during interview. Regarding

the Alzheimer's Disease Neuroimaging Initiative (ADNI) dataset, neurologists from multiple cooperation institutes made the AD diagnosis. Consistent with previous studies, we dichotomized AD patients into early- and late-onset groups (age at onset <65 or ≥ 65 years, respectively) [8, 14]. All participants underwent the evaluations of Mini-Mental State Examination (MMSE) and neuropsychological battery, involving Wechsler Memory Scale-logical memory (WMS-LM), delayed recall, language (Semantic verbal fluency, SVF), attention (Trail Making Test, Part A, TMT-A), and executive function (Trail Making Test, Part B, TMT-B). Additionally, dementia severity and depression severity were assessed based on Clinical Dementia Rating (CDR) and the Geriatric Depression Scale (GDS).

We divided healthy elderly controls into younger and older group based on their age (YHC/OHC, age <65 or ≥ 65 years, respectively). Notably, age, education, and sex of YHC and OHC were matched to their corresponding patient group respectively. In both datasets, we defined YHC and OHC as having a CDR of 0, an MMSE between 24 and 30 (inclusive), a WMS-LM, delayed recall (≥ 9 for subjects having ≥ 16 years education; ≥ 5 for subjects having 8–15 years education; and ≥ 3 for subjects having ≤ 7 years education); absence of clinical depression (GDS < 6) and dementia symptom. We excluded subjects with following conditions: significant neurological, psychiatric, and medical illness; severe head trauma history [40]; taking non-AD-related medication that may potentially influence cerebral function; clinical depression; drug or alcohol abuse.

Finally, we identified 31 EOAD, 45 LOAD, 64 YHC, and 46 OHC from the ZJU dataset (Table 1), as well as 17 EOAD, 30 LOAD, 31 YHC, and 34 OHC from the ADNI dataset (Supplementary Material 1**)**.

MR imaging acquisition

In both databases, researchers used foam padding and earplugs to limit head motion and reduce scanner noise. Regarding the ZJU database, MRI data were acquired from the 3.0 Tesla scanner (GE Discover 750) using an 8-channel head coil. We acquired the T1-weighted structural images based on the fast-spoiled gradient-echo sequence with TR = 7.3 ms, TE = 3.0 ms; slice number = 196; FOV=256 ×256; voxel size=1.02 ×mm ×1.02 ×mm 1.2×mm; flip angle = 11°; and bandwidth = 244.141 Hz/pix. DWI data were acquired using a single shot, diffusion-weighted spin-echo echo-planar imaging sequence. Specifically, images were acquired using b = 1,000 s/mm^2 in 30 directions; 5 volumes were acquired without diffusion weighting (b-value = 0 s/mm^2). Other parameters of DTI were as follows: TR/TE = 8,000/80.8 ms, flip angle = 90°, slice thickness = 2 mm without slice gap, matrix size = 128 × 128, FOV = 256 × 256.

Regarding ADNI database, each subject underwent MRI scanning based on the ADNI protocol using the GE 3.0 Tesla scanner across 14 institute sites. The sequence of T1-weighted structural imaging is IR-SPGR sequence with following parameters: repetition time (TR) = 6.96 ms, echo time (TE) = 2.8 ms, Invert time (TI) = 400 ms, field of view (FOV) = 256 × 256, voxel size=1.02 mm × 1.02 mm × 1.2mm, flip angle = 11°. Diffusion-weighted imaging (DWI) data were acquired using the Echo Planar Imaging (EPI) sequence with 41 directions and the following specifications: slice number = 59, acquisition matrix = 256 × 256, voxel size= 1.4 mm × 1.4 mm × 2.7 mm, flip angle= 90°, with 41 diffusion-weighted images (b = 1000 s/mm^2) and 5 non-diffusion weighted images (b = 0 s/mm^2). Across 14 sites, the TR was the range from 12500 to 13000 ms.

DWI pre-processing and Fixel-based analysis

The DWI data pre-processing and fixel-based analysis were performed using MRtrix3 (https://www.mrtrix.org) [41]. The DWI were denoised then corrected for eddy-current, head motion, and bias field; then, we normalized intensity across subjects. An average response function was firstly generated by averaging all subjects' single fiber response function before the FBA. Then, fiber orientation distributions were estimated using constrained spherical deconvolution, and we applied multi-shell multi-tissue constrained spherical deconvolution to obtain more robust outcomes [42]. From between-group comparisons, we generated fiber orientation distributions template of young subjects based on randomly selected 10 EOAD and 10 YHC. Similarly, we generated the template for each elder subject. Then the fiber orientation distributions in the template were segmented to fixels for generating the fixel template analysis mask. For spatial correspondence, the fiber orientation distributions image of each subject was transformed into the corresponding template. Then we used the resulting local transformations to segment and reorient fixels to match the template in each voxel. Finally, we assigned FD, FC, and FDC to fixels in the template space.

To facilitate connectivity-based fixel enhancement, whole-brain probabilistic tractography was performed on a group-wised template of fiber orientation distributions. A total of 20 million streamlines was generated and filtered to 2 million for reducing reconstruction biases using the spherical deconvolution informed filtering of tractograms algorithm [43].

Table 1. Clinical and demographic data of the ZJU database.

Group	YHC	EOAD	OHC	LOAD	Interaction		ANOVA	
	n=64	n=31	n=46	n=45	F/χ^2	p	F/χ^2	p
Age	59.7 (2.5)	60.8 (3.3)	72.4 (3.8)	74.3 (4.6)	0.7	0.4	86.9	**<0.001**
Education	10.7 (3.7)	9.4 (2.9)	10.5 (4.1)	10.5 (4.0)	2.6	0.1	0.9	0.4
Sex, F/M	38/26	21/10	22/24	23/22	0.1	0.8	3.7	0.3
GDS	1.9 (2.5)	1.6 (1.5)	1.2 (1.6)	1.4 (1.2)	0.7	0.4	1.2	0.3
CDR global	0 (0)	1.1 (0.3)ł	0 (0)	1.0 (0.5)ǂ	0.2	0.6	220.9	**<0.001**
CDR sum	0 (0)	4.9 (2.1)ł	0 (0.1)	4.7 (3.6)ǂ	0.1	0.7	87	**<0.001**
MMSE	28.1 (1.6)	20.6 (3.6)ł	28.3 (1.5)	20.0 (3.7)ǂ	0.7	0.4	140	**<0.001**
LM delay	8.5 (4.3)	0.6 (1.3)ł	8.6 (3.7)	0.3 (0.7)ǂ	0.01	0.9	96	**<0.001**
TMT-A	69.2 (28.2)	98.3 (40.6)ł	70.8 (29.8)	106.3 (38.0)ǂ	0.4	0.6	16.5	**<0.001**
TMT-B	172.6 (64.3)	223.6 (90.6)ł	181.5 (69.8)	250.3 (83.4)ǂ	0.1	0.7	17.8	**<0.001**
SVF	16.3 (3.9)	11.0 (5.3)ł	16.0 (4.8)	8.9 (5.0)ǂ	3.6	0.1	31.3	**<0.001**
CDT	4.1 (0.7)	3.2 (0.6)ł	4.3 (0.6)	3.3 (0.6)ǂ	0.2	0.7	33.6	**<0.001**

ł and ǂ Represent the significant difference between YHC and OHC, as well as EOAD and LOAD ($p<0.05$), respectively. Interactive effects comprise the factors of onset age (<65 or ≥65 years) and disease status (controls or patients). Abbreviations: YHC, young healthy controls; EOAD, early-onset Alzheimer's disease; OHC, old healthy controls; LOAD, late-onset Alzheimer's disease; CDR global/sum, Clinical Dementia Rating, global score and sum score of box; MMSE, Mini-Mental State Examination; GDS, Geriatric Depression Scale; LM, Logical Memory; TMT-A/B, Trail Making Test, part A/B; SVF, Semantic Verbal Fluency.

PET image data

Based on predefined regions of interest (ROI), standardized update value ratios (SUVRs) were calculated using the mean signal of the whole cerebellar (florbetapir) and cerebellar cortex (flortaucipir) as the reference region [44]. We chose 4 ROI, including the SUVRs of composite amyloid deposition and Tau from Braak stage I/II, III/IV, and V/VI (Supplementary Material 5) [45].

White matter hyperintensities assessment

Recently, increasing evidence shows that AD is a multifactorial disease with multiple contributors, including cerebrovascular disease [21]. Considering that WMH is the typical imaging marker of CSVD [46], we measured the WMH burden of each subject using a semi-quantitative scoring method developed by Fazekas et al. [47].

Statistical analysis

Analysis of demographics

We performed multiple statistical analyses on demographic data using SPSS (Version 23). Continuous variables were compared between groups using two-sample T-tests. Group differences in categorical variables were assessed using Fisher's exact test.

Fixel-based analysis

The FD, FC, and FDC of each subject in the fixel level (FWE corrected, P-values < 0.05, 5000 permutations, controlling age and sex) were compared between groups. We then performed connectivity-based smoothing and statistical inference using CFE (smoothing = 10 mm full-width at half-maximum, C = 0.5, E = 2, H = 3) [48]. Significant streamlines were color-coded by the effect size (percentage) relative to their corresponding controls.

Tract-based analysis and correlation analysis

Based on previous literature, we focused on 12 tracts which are susceptible to AD-related pathologies, including the splenium of corpus callosum (SCC), fornix column and body, bilateral dorsal and ventral cingulum, inferior longitudinal fasciculus/inferior frontal-occipital fasciculus (ILF/IFOF), posterior thalamic radiation (PTR), and fornix-hippocampus [14, 18, 49, 50]. Then, we extracted the mean FD, FC, and FDC values from these pre-defined tracts and used two-sample t-tests to assess the differences of fixel-based analysis metrics between AD patients and counterpart, controlling for age and sex (Bonferroni-corrected, P-value < 0.05).

Furthermore, we explored the correlation between mean fixel-based analysis metrics and cognitive performances, as well as PET biomarkers. Given the

explorative nature of our work, statistical significance is defined as p-value < 0.001 (uncorrected) controlling for age and sex.

Ethics approval and patient consent statement

Regarding the ZJU database, our study was approved by the Review Board of the Second Affiliated Hospital, Zhejiang University School of Medicine, and conducted following the Declaration of Helsinki. We obtained the written informed consent from all participants. Regarding the ADNI database, this project was approved by the Institutional Review Boards of all participating institutions, and all of the participating institutions, and informed written consent was obtained from all participants at each site. More information could be found in http://adni.loni.usc.edu/.

Abbreviations

FD: fiber density; FC: fiber bundle cross-section; FDC: fiber density and bundle cross-section; EOAD: early-onset Alzheimer's disease; LOAD: late-onset Alzheimer's disease; YHC: young healthy controls; OHC: old healthy controls.

AUTHOR CONTRIBUTIONS

Xiao Luo and Shuyue Wang designed the study and writing work. Peiyu Huang and MM Zhang contributed to data analysis and draft modification. YJ, KCL, QZZ, HH, XJG, TG, CW, RTZ, JZ, DW, XPX, Peiyu Huang contributed to the data collection and discussion. All authors read and approved the final manuscript.

CONFLICTS OF INTEREST

The authors declare that they have no conflicts of interest.

FUNDING

This study was funded by the National Natural Science Foundation of China (Grant NO. 81901707/82001766), Zhejiang Medicine Health Science and Technology Program (Grant NO. 2021432939) the National Key Research and Development Program of China (NO. 2016YFC1306600).

We thank the patients, researchers, and clinicians involved in the ZJU database. Data collection and sharing for our work was also supported by the Alzheimer's Disease Neuroimaging Initiative (ADNI) (National Institutes of Health Grant U01 AG024904) and DOD ADNI (Department of Defense award number W81XWH-12-2-0012).

REFERENCES

1. Renvoize E, Hanson M, Dale M. Prevalence and causes of young onset dementia in an English health district. Int J Geriatr Psychiatry. 2011; 26:106–07. https://doi.org/10.1002/gps.2456 PMID:21157856

2. Koedam EL, Pijnenburg YA, Deeg DJ, Baak MM, van der Vlies AE, Scheltens P, van der Flier WM. Early-onset dementia is associated with higher mortality. Dement Geriatr Cogn Disord. 2008; 26:147–52. https://doi.org/10.1159/000149585 PMID:18679029

3. Smits LL, Pijnenburg YA, Koedam EL, van der Vlies AE, Reuling IE, Koene T, Teunissen CE, Scheltens P, van der Flier WM. Early onset Alzheimer's disease is associated with a distinct neuropsychological profile. J Alzheimers Dis. 2012; 30:101–08. https://doi.org/10.3233/JAD-2012-111934 PMID:22366769

4. Joubert S, Gour N, Guedj E, Didic M, Guériot C, Koric L, Ranjeva JP, Felician O, Guye M, Ceccaldi M. Early-onset and late-onset Alzheimer's disease are associated with distinct patterns of memory impairment. Cortex. 2016; 74:217–32. https://doi.org/10.1016/j.cortex.2015.10.014 PMID:26694580

5. Schöll M, Ossenkoppele R, Strandberg O, Palmqvist S, Jögi J, Ohlsson T, Smith R, Hansson O, and Swedish BioFINDER study. Distinct 18F-AV-1451 tau PET retention patterns in early- and late-onset Alzheimer's disease. Brain. 2017; 140:2286–94. https://doi.org/10.1093/brain/awx171 PMID:29050382

6. Cho H, Seo SW, Kim JH, Suh MK, Lee JH, Choe YS, Lee KH, Kim JS, Kim GH, Noh Y, Ye BS, Kim HJ, Yoon CW, et al. Amyloid deposition in early onset versus late onset Alzheimer's disease. J Alzheimers Dis. 2013; 35:813–21. https://doi.org/10.3233/JAD-121927 PMID:23507771

7. Choo IH, Lee DY, Kim JW, Seo EH, Lee DS, Kim YK, Kim SG, Park SY, Woo JI, Yoon EJ. Relationship of amyloid-β burden with age-at-onset in Alzheimer disease. Am J Geriatr Psychiatry. 2011; 19:627–34. https://doi.org/10.1097/JGP.0b013e318202bf3a PMID:21709608

8. Cho H, Choi JY, Lee SH, Lee JH, Choi YC, Ryu YH, Lee MS, Lyoo CH. Excessive tau accumulation in the parieto-occipital cortex characterizes early-onset Alzheimer's disease. Neurobiol Aging. 2017; 53:103–11. https://doi.org/10.1016/j.neurobiolaging.2017.01.024 PMID:28254589

9. Ossenkoppele R, Zwan MD, Tolboom N, van Assema DM, Adriaanse SF, Kloet RW, Boellaard R, Windhorst AD, Barkhof F, Lammertsma AA, Scheltens P, van der Flier WM, van Berckel BN. Amyloid burden and metabolic function in early-onset Alzheimer's disease: parietal lobe involvement. Brain. 2012; 135:2115–25. https://doi.org/10.1093/brain/aws113 PMID:22556189

10. Liu Y, Spulber G, Lehtimäki KK, Könönen M, Hallikainen I, Gröhn H, Kivipelto M, Hallikainen M, Vanninen R, Soininen H. Diffusion tensor imaging and tract-based spatial statistics in Alzheimer's disease and mild cognitive impairment. Neurobiol Aging. 2011; 32:1558–71. https://doi.org/10.1016/j.neurobiolaging.2009.10.006 PMID:19913331

11. Agosta F, Pievani M, Sala S, Geroldi C, Galluzzi S, Frisoni GB, Filippi M. White matter damage in Alzheimer disease and its relationship to gray matter atrophy. Radiology. 2011; 258:853–63. https://doi.org/10.1148/radiol.10101284 PMID:21177393

12. Liu J, Liang P, Yin L, Shu N, Zhao T, Xing Y, Li F, Zhao Z, Li K, Han Y. White matter abnormalities in two different subtypes of amnestic mild cognitive impairment. PLoS One. 2017; 12:e0170185. https://doi.org/10.1371/journal.pone.0170185 PMID:28107493

13. Shu N, Wang X, Bi Q, Zhao T, Han Y. Disrupted topologic efficiency of white matter structural connectome in individuals with subjective cognitive decline. Radiology. 2018; 286:229–38. https://doi.org/10.1148/radiol.2017162696 PMID:28799862

14. Canu E, Agosta F, Spinelli EG, Magnani G, Marcone A, Scola E, Falautano M, Comi G, Falini A, Filippi M. White matter microstructural damage in Alzheimer's disease at different ages of onset. Neurobiol Aging. 2013; 34:2331–40. https://doi.org/10.1016/j.neurobiolaging.2013.03.026 PMID:23623599

15. Jeurissen B, Leemans A, Tournier JD, Jones DK, Sijbers J. Investigating the prevalence of complex fiber configurations in white matter tissue with diffusion magnetic resonance imaging. Hum Brain Mapp. 2013; 34:2747–66. https://doi.org/10.1002/hbm.22099 PMID:22611035

16. Raffelt DA, Tournier JD, Smith RE, Vaughan DN, Jackson G, Ridgway GR, Connelly A. Investigating white matter fibre density and morphology using fixel-based analysis. Neuroimage. 2017; 144:58–73. https://doi.org/10.1016/j.neuroimage.2016.09.029 PMID:27639350

17. Li Y, Guo T, Guan X, Gao T, Sheng W, Zhou C, Wu J, Xuan M, Gu Q, Zhang M, Yang Y, Huang P. Fixel-based analysis reveals fiber-specific alterations during the progression of Parkinson's disease. Neuroimage Clin. 2020; 27:102355. https://doi.org/10.1016/j.nicl.2020.102355 PMID:32736325

18. Mito R, Raffelt D, Dhollander T, Vaughan DN, Tournier JD, Salvado O, Brodtmann A, Rowe CC, Villemagne VL, Connelly A. Fibre-specific white matter reductions in Alzheimer's disease and mild cognitive impairment. Brain. 2018; 141:888–902. https://doi.org/10.1093/brain/awx355 PMID:29309541

19. Raffelt D, Tournier JD, Rose S, Ridgway GR, Henderson R, Crozier S, Salvado O, Connelly A. Apparent fibre density: a novel measure for the analysis of diffusion-weighted magnetic resonance images. Neuroimage. 2012; 59:3976–94. https://doi.org/10.1016/j.neuroimage.2011.10.045 PMID:22036682

20. Sánchez SM, Duarte-Abritta B, Abulafia C, De Pino G, Bocaccio H, Castro MN, Sevlever GE, Fonzo GA, Nemeroff CB, Gustafson DR, Guinjoan SM, Villarreal MF. White matter fiber density abnormalities in cognitively normal adults at risk for late-onset Alzheimer's disease. J Psychiatr Res. 2020; 122:79–87. https://doi.org/10.1016/j.jpsychires.2019.12.019 PMID:31931231

21. Sweeney MD, Montagne A, Sagare AP, Nation DA, Schneider LS, Chui HC, Harrington MG, Pa J, Law M, Wang DJ, Jacobs RE, Doubal FN, Ramirez J, et al. Vascular dysfunction-the disregarded partner of Alzheimer's disease. Alzheimers Dement. 2019; 15:158–67. https://doi.org/10.1016/j.jalz.2018.07.222 PMID:30642436

22. Finsterwalder S, Vlegels N, Gesierich B, Araque Caballero MÁ, Weaver NA, Franzmeier N, Georgakis MK, Konieczny MJ, Koek HL, Karch CM, Graff-Radford NR, Salloway S, Oh H, et al, and Dominantly Inherited Alzheimer Network (DIAN), and DELCODE study group, and Alzheimer's Disease Neuroimaging Initiative (ADNI), and Utrecht VCI study group. Small vessel disease more than Alzheimer's disease determines diffusion MRI alterations in memory clinic patients. Alzheimers Dement. 2020; 16:1504–14. https://doi.org/10.1002/alz.12150 PMID:32808747

23. Murray ME, Graff-Radford NR, Ross OA, Petersen RC, Duara R, Dickson DW. Neuropathologically defined subtypes of Alzheimer's disease with distinct clinical

characteristics: a retrospective study. Lancet Neurol. 2011; 10:785–96.
https://doi.org/10.1016/S1474-4422(11)70156-9
PMID:21802369

24. Greicius MD, Supekar K, Menon V, Dougherty RF. Resting-state functional connectivity reflects structural connectivity in the default mode network. Cereb Cortex. 2009; 19:72–8.
https://doi.org/10.1093/cercor/bhn059
PMID:18403396

25. Hau J, Sarubbo S, Perchey G, Crivello F, Zago L, Mellet E, Jobard G, Joliot M, Mazoyer BM, Tzourio-Mazoyer N, Petit L. Cortical terminations of the inferior fronto-occipital and uncinate fasciculi: anatomical stem-based virtual dissection. Front Neuroanat. 2016; 10:58.
https://doi.org/10.3389/fnana.2016.00058
PMID:27252628

26. Gour N, Felician O, Didic M, Koric L, Gueriot C, Chanoine V, Confort-Gouny S, Guye M, Ceccaldi M, Ranjeva JP. Functional connectivity changes differ in early and late-onset Alzheimer's disease. Hum Brain Mapp. 2014; 35:2978–94.
https://doi.org/10.1002/hbm.22379
PMID:24123475

27. Adriaanse SM, Binnewijzend MA, Ossenkoppele R, Tijms BM, van der Flier WM, Koene T, Smits LL, Wink AM, Scheltens P, van Berckel BN, Barkhof F. Widespread disruption of functional brain organization in early-onset Alzheimer's disease. PLoS One. 2014; 9:e102995.
https://doi.org/10.1371/journal.pone.0102995
PMID:25080229

28. Lehmann M, Madison C, Ghosh PM, Miller ZA, Greicius MD, Kramer JH, Coppola G, Miller BL, Jagust WJ, Gorno-Tempini ML, Seeley WW, Rabinovici GD. Loss of functional connectivity is greater outside the default mode network in nonfamilial early-onset Alzheimer's disease variants. Neurobiol Aging. 2015; 36:2678–86.
https://doi.org/10.1016/j.neurobiolaging.2015.06.029
PMID:26242705

29. Li KC, Luo X, Zeng QZ, Xu XJ, Huang PY, Shen ZJ, Xu JJ, Zhou J, Zhang MM. Distinct patterns of interhemispheric connectivity in patients with early- and late-onset Alzheimer's disease. Front Aging Neurosci. 2018; 10:261.
https://doi.org/10.3389/fnagi.2018.00261
PMID:30237764

30. Jokinen H, Ryberg C, Kalska H, Ylikoski R, Rostrup E, Stegmann MB, Waldemar G, Madureira S, Ferro JM, van Straaten EC, Scheltens P, Barkhof F, Fazekas F, et al, and LADIS Group. Corpus callosum atrophy is associated with mental slowing and executive deficits in subjects with age-related white matter hyperintensities: the LADIS study. J Neurol Neurosurg Psychiatry. 2007; 78:491–96.
https://doi.org/10.1136/jnnp.2006.096792
PMID:17028118

31. Menegaux A, Meng C, Neitzel J, Bäuml JG, Müller HJ, Bartmann P, Wolke D, Wohlschläger AM, Finke K, Sorg C. Impaired visual short-term memory capacity is distinctively associated with structural connectivity of the posterior thalamic radiation and the splenium of the corpus callosum in preterm-born adults. Neuroimage. 2017; 150:68–76.
https://doi.org/10.1016/j.neuroimage.2017.02.017
PMID:28188917

32. McAleese KE, Firbank M, Dey M, Colloby SJ, Walker L, Johnson M, Beverley JR, Taylor JP, Thomas AJ, O'Brien JT, Attems J. Cortical tau load is associated with white matter hyperintensities. Acta Neuropathol Commun. 2015; 3:60.
https://doi.org/10.1186/s40478-015-0240-0
PMID:26419828

33. Mielke MM, Okonkwo OC, Oishi K, Mori S, Tighe S, Miller MI, Ceritoglu C, Brown T, Albert M, Lyketsos CG. Fornix integrity and hippocampal volume predict memory decline and progression to Alzheimer's disease. Alzheimers Dement. 2012; 8:105–13.
https://doi.org/10.1016/j.jalz.2011.05.2416
PMID:22404852

34. Stern Y, Arenaza-Urquijo EM, Bartrés-Faz D, Belleville S, Cantilon M, Chetelat G, Ewers M, Franzmeier N, Kempermann G, Kremen WS, Okonkwo O, Scarmeas N, Soldan A, et al, and the Reserve, Resilience and Protective Factors PIA Empirical Definitions and Conceptual Frameworks Workgroup. Whitepaper: defining and investigating cognitive reserve, brain reserve, and brain maintenance. Alzheimers Dement. 2020; 16:1305–11.
https://doi.org/10.1016/j.jalz.2018.07.219
PMID:30222945

35. Choy SW, Bagarinao E, Watanabe H, Ho ET, Maesawa S, Mori D, Hara K, Kawabata K, Yoneyama N, Ohdake R, Imai K, Masuda M, Yokoi T, et al. Changes in white matter fiber density and morphology across the adult lifespan: a cross-sectional fixel-based analysis. Hum Brain Mapp. 2020; 41:3198–211.
https://doi.org/10.1002/hbm.25008 PMID:32304267

36. Araque Caballero MÁ, Suárez-Calvet M, Duering M, Franzmeier N, Benzinger T, Fagan AM, Bateman RJ, Jack CR, Levin J, Dichgans M, Jucker M, Karch C, Masters CL, et al. White matter diffusion alterations precede symptom onset in autosomal dominant Alzheimer's disease. Brain. 2018; 141:3065–80.
https://doi.org/10.1093/brain/awy229
PMID:30239611

37. Verhelst H, Giraldo D, Vander Linden C, Vingerhoets G, Jeurissen B, Caeyenberghs K. Cognitive training in young patients with traumatic brain injury: a fixel-based analysis. Neurorehabil Neural Repair. 2019; 33:813–24. https://doi.org/10.1177/1545968319868720 PMID:31416407

38. Cousineau M, Jodoin PM, Morency FC, Rozanski V, Grand'Maison M, Bedell BJ, Descoteaux M. A test-retest study on Parkinson's PPMI dataset yields statistically significant white matter fascicles. Neuroimage Clin. 2017; 16:222–33. https://doi.org/10.1016/j.nicl.2017.07.020 PMID:28794981

39. Jack CR Jr, Bennett DA, Blennow K, Carrillo MC, Dunn B, Haeberlein SB, Holtzman DM, Jagust W, Jessen F, Karlawish J, Liu E, Molinuevo JL, Montine T, et al, and Contributors. NIA-AA Research Framework: toward a biological definition of Alzheimer's disease. Alzheimers Dement. 2018; 14:535–62. https://doi.org/10.1016/j.jalz.2018.02.018 PMID:29653606

40. Sun Y, Wang X, Wang Y, Dong H, Lu J, Scheininger T, Ewers M, Jessen F, Zuo XN, Han Y. Anxiety correlates with cortical surface area in subjective cognitive decline: APOE ε4 carriers versus APOE ε4 non-carriers. Alzheimers Res Ther. 2019; 11:50. https://doi.org/10.1186/s13195-019-0505-0 PMID:31159873

41. Tournier JD, Smith R, Raffelt D, Tabbara R, Dhollander T, Pietsch M, Christiaens D, Jeurissen B, Yeh CH, Connelly A. MRtrix3: a fast, flexible and open software framework for medical image processing and visualisation. Neuroimage. 2019; 202:116137. https://doi.org/10.1016/j.neuroimage.2019.116137 PMID:31473352

42. Jeurissen B, Tournier JD, Dhollander T, Connelly A, Sijbers J. Multi-tissue constrained spherical deconvolution for improved analysis of multi-shell diffusion MRI data. Neuroimage. 2014; 103:411–26. https://doi.org/10.1016/j.neuroimage.2014.07.061 PMID:25109526

43. Smith RE, Tournier JD, Calamante F, Connelly A. SIFT: spherical-deconvolution informed filtering of tractograms. Neuroimage. 2013; 67:298–312. https://doi.org/10.1016/j.neuroimage.2012.11.049 PMID:23238430

44. Landau SM, Lu M, Joshi AD, Pontecorvo M, Mintun MA, Trojanowski JQ, Shaw LM, Jagust WJ, and Alzheimer's Disease Neuroimaging Initiative. Comparing positron emission tomography imaging and cerebrospinal fluid measurements of β-amyloid. Ann Neurol. 2013; 74:826–36. https://doi.org/10.1002/ana.23908 PMID:23536396

45. Braak H, Braak E. Neuropathological stageing of Alzheimer-related changes. Acta Neuropathol. 1991; 82:239–59. https://doi.org/10.1007/BF00308809 PMID:1759558

46. Wardlaw JM, Smith C, Dichgans M. Small vessel disease: mechanisms and clinical implications. Lancet Neurol. 2019; 18:684–96. https://doi.org/10.1016/S1474-4422(19)30079-1 PMID:31097385

47. Fazekas F, Chawluk JB, Alavi A, Hurtig HI, Zimmerman RA. MR signal abnormalities at 1.5 T in Alzheimer's dementia and normal aging. AJR Am J Roentgenol. 1987; 149:351–56. https://doi.org/10.2214/ajr.149.2.351 PMID:3496763

48. Raffelt DA, Smith RE, Ridgway GR, Tournier JD, Vaughan DN, Rose S, Henderson R, Connelly A. Connectivity-based fixel enhancement: whole-brain statistical analysis of diffusion MRI measures in the presence of crossing fibres. Neuroimage. 2015; 117:40–55. https://doi.org/10.1016/j.neuroimage.2015.05.039 PMID:26004503

49. Canu E, Frisoni GB, Agosta F, Pievani M, Bonetti M, Filippi M. Early and late onset Alzheimer's disease patients have distinct patterns of white matter damage. Neurobiol Aging. 2012; 33:1023–33. https://doi.org/10.1016/j.neurobiolaging.2010.09.021 PMID:21074899

50. Zhao W, Wang X, Yin C, He M, Li S, Han Y. Trajectories of the hippocampal subfields atrophy in the Alzheimer's disease: a structural imaging study. Front Neuroinform. 2019; 13:13. https://doi.org/10.3389/fninf.2019.00013 PMID:30983985

SUPPLEMENTARY MATERIALS

Supplementary Materials 1

Participants' information

Introduction of database of Zhejiang University and Alzheimer's Disease Neuroimaging Initiative

Regarding the Zhejiang University (ZJU) database, we recruited participants from the Second Affiliated Hospital of Zhejiang University School of Medicine, Zhejiang Province, P.R.China. This database was established in 2012. Alzheimer's disease (AD) and mild cognitive impairment patients were recruited from the memory clinics by neurologists, and healthy controls were recruited from the spouses of patients or community advertisements. Participants from the ZJU databased are entirely composed of the Chinese Han population, while participants from the ADNI database are mainly composed of the Caucasian population.

Each participant from the database of ZJU and ADNI underwent a comprehensive cognitive scale, blood collection, and multiple sequence MRI scanning [1]. Further, in the ADNI database, 13 out of 17 EOAD (76.5%), 27 out of 30 LOAD (90.0%), 12 out of 31 YHC (38.7%), and 32 out of 34 OHC (94.1%) had florbetapir PET data; 6 out of 17 EOAD (35.3%), 18 out of 31 YHC (58.1%), and 16 out of 34 OHC (47.0%) had flortaucipir-PET data. We aim to explore the neurobiological mechanisms of EOAD and find early AD imaging biomarkers.

Demographics

All participants underwent the evaluations of Mini-Mental State Examination (MMSE) [2] and neuropsychological battery, involving Wechsler Memory Scale-logical memory (WMS-LM), delayed recall, language (Semantic verbal fluency, SVF), attention (Trail Making Test, Part A, TMT-A), and executive function (Trail Making Test, Part B, TMT-B). Additionally, dementia severity and depression severity were assessed based on Clinical Dementia Rating (CDR) [3] and the Geriatric Depression Scale (GDS) [4]. In both databases, early-onset Alzheimer's disease (EOAD) and young healthy controls (YHC) matched late-onset Alzheimer's disease (LOAD) and old healthy controls (OHC), respectively, for the age, gender, education, general cognitive ability (reflected by MMSE), and disease severity (reflected by Clinical Dementia Rating, CDR). Notably, the interval between the behavioral scale and the MRI scan should not exceed one week for the ZJU database, and three months for the ADNI database.

In the ZJU database, the diagnosis of probable AD was made by an experienced neurologist according to the

Supplementary Table 1. Demographics of the groups in the ADNI database.

Group	YHC	EOAD	OHC	LOAD	Interaction		ANOVA	
	n=31	n=17	n=34	n=30	F/χ^2	p	F/χ^2	p
Age	61.9 (2.4)	61.2 (2.6)	74.4 (4.5)	76.8 (5.3)	0.7	0.4	107.6	**<0.001**
Education	16.6 (2.4)	15.5 (2.9)	16.2 (3.7)	15.4 (3.0)	0.5	0.5	0.9	0.4
Sex, F/M	23/8	11/6	22/12	11/19	0.04	0.8	9.9	**0.02***
GDS	0.6 (0.7)	2.4 (1.1)ł	0.9 (1.3)	1.9 (1.6)ǂ	0.6	0.4	11.9	**<0.001**
CDR global	0 (0)	0.8 (0.2)ł	0 (0)	0.9 (0.2)ǂ	0.1	0.8	272.6	**<0.001**
CDR sum	0 (0.1)	3.9 (2.2)ł	0.1 (0.2)	4.6 (1.6)ǂ	1.1	0.3	120.4	**<0.001**
MMSE	29.2 (0.8)	24.6 (3.8)ł	29.2 (1.0)	23.1 (1.9)ǂ	1.6	0.2	78.6	**<0.001**
LM delay	13.7 (3.9)	5.4 (3.7)ł	12.8 (3.0)	1.2 (1.6)ǂ	3.9	0.1	82.6	**<0.001**
TMT-A	28.7 (6.1)	64.4 (42.3)ł	35.9 (8.4)	53.3 (26.7)ǂ	0.04	0.9	9.6	**<0.001**
TMT-B	62.6 (17.1)	170.5 (99.6)ł	84.5 (34.7)	206.9 (95.7)ǂ	1.3	0.3	24.5	**<0.001**
SVF	24.4 (4.3)	16.4 (6.3)ł	20.5 (5.0)	12.4 (4.9)ǂ	0.005	0.9	25	**<0.001**
CDT	4.8 (0.4)	3.7 (1.6)ł	4.7 (0.6)	3.8 (1.2)ǂ	0.4	0.6	7.7	**<0.001**

ł and ǂ Represent the significant difference between YHC and OHC, as well as EOAD and LOAD ($p<0.05$), respectively. Interactive effects comprise the factors of onset age (<65 or ≥65 years) and disease status (controls or patients). Abbreviations: YHC, young healthy controls; EOAD, early-onset Alzheimer's disease; OHC, old healthy controls; LOAD, late-onset Alzheimer's disease; CDR global/sum, Clinical Dementia Rating, global score and sum score of box; MMSE, Mini-Mental State Examination; GDS, Geriatric Depression Scale; LM, Logical Memory; TMT-A/B, Trail Making Test, part A/B; SVF, Semantic Verbal Fluency.

NINCDS/ADRDA (National Institute of Neurological and Communicative Disorders and Stroke and the Alzheimer's Disease and Related Disorders Association) criteria [5]. Additionally, the neurologist also evaluated the neurological history, blood biochemical examination, and neuropsychological scales to exclude dementia from other causes. The age of disease onset was identified by the interview conducted with the patient's family members or caregivers. Regarding the ADNI database, neurologists from multiple cooperation institutes made the AD diagnosis. We downloaded the "diagnosis summary" from LONI (https://ida.loni.usc.edu) in 2018 July. Consistent with previous studies, we dichotomized AD patients into early- and late-onset groups (age at onset <65 or ≥ 65 years, respectively) [6, 7].

In both databases, we defined YHC and OHC as having a CDR of 0, an MMSE between 24 and 30 (inclusive), a WMS-LM, delayed recall (≥ 9 for subjects having ≥ 16 years education; ≥ 5 for subjects having 8-15 years education; and ≥ 3 for subjects having ≤ 7 years education); absence of clinical depression (GDS < 6) and dementia symptom. Further, we excluded subjects with the following manifestations: significant neurological, psychiatric, and medical illness; severe head trauma history; application of non-AD-related medication potentially influence cerebral function; clinical depression; drug or alcohol abuse.

Supplementary Materials 2

Repeated FBA based on the matched sample size of both databases

Due to the differences in the sample sizes of two independent databases, different statistical effects may contribute to the repeated result difference between databases. To eliminate the potential factor, we compressed the sample of the ZJU database to the same size as the ADNI database. There is still no significant differences in age, gender, education, general cognitive, and disease severity between groups of patients and controls in the compressed ZJU database. Then, we re-performed a whole brain-based FBA in the ZJU database after sample reduction (FWE-corrected, $p < 0.05$, 5000 permutations) [8].

Although the affected regions got smaller, the trend of results remained unchanged. We found that EOAD had widespread FD decreases in the splenium of corpus callosum (SCC), left fornix-HP, and bilateral dorsal and ventral cingulum relative to YHC. Additionally, EOAD had an FC decrease in the bilateral dorsal cingulum relative to YHC. Regarding the FDC, we found that EOAD patients had a widespread decrease in the bilateral dorsal and ventral cingulum, and left fornix-HP relative to YHC. By contrast, we found that LOAD patients had a marked FD decrease in the bilateral ventral cingulum and FC decrease in bilateral dorsal and ventral cingulum relative to OHC. No difference in FDC existed between LOAD and ONC.

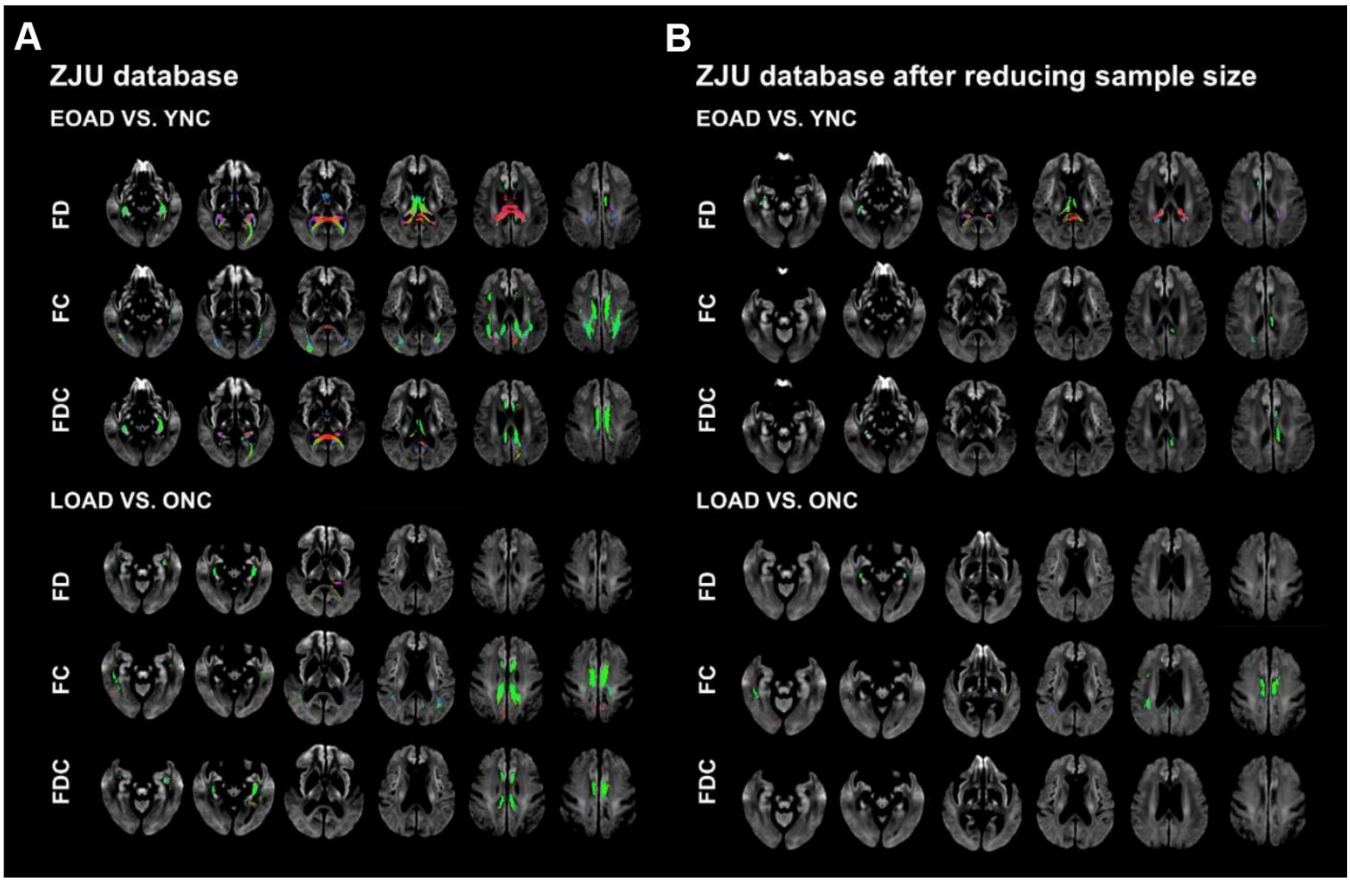

Supplementary Figure 1. The fiber tract-specific reduction in EOAD/LOAD versus controls from whole-brain FBA. (**A**, **B**) Represent results from the database of ZJU and ZJU after sample reduction, respectively. We color-coded the significant streamlines (patients versus controls) by streamline orientation (left-right: red; inferior-superior: blue; anterior-posterior: green). Abbreviation: FBA, fixel-based analysis; FD, fiber density; FC, fiber bundle cross-section; FDC, fiber density and bundle cross-section.

Supplementary Table 2. Demographics of ZJU database after sample reduction.

Group	YHC	EOAD	OHC	LOAD	Interaction		ANOVA	
	n=31	n=17	n=34	n=30	F/χ^2	p	F/χ^2	p
Age	62.1 (1.6)	61.2 (2.3)	74.9 (3.7)	76.1 (3.0)	3.5	0.06	206	**<0.001**
Education	11.0 (4.0)	10.6 (3.0)	10.6 (4.2)	10.8 (4.0)	0.1	0.7	0.1	0.9
Sex, F/M	18/13	10/7	15/19	16/14	0.2	0.7	1.6	0.7
GDS	1.6 (1.9)	1.7 (1.8)	1.1 (1.6)	1.3 (1.1)	0.01	0.9	0.8	0.5
CDR global	0 (0)	1.0 (0.3)	0 (0)	1.0 (0.5)	0.1	0.8	138.7	**<0.001**
CDR sum	0 (0)	4.7 (2.4)	0 (0.1)	4.5 (3.5)	0.1	0.8	47.0	**<0.001**
MMSE	28.3 (1.6)	21.1 (3.1)	28.4 (1.6)	20.2 (3.6)	0.9	0.3	89.0	**<0.001**
LM delay	8.1 (4.2)	0.6 (1.5)	8.2 (3.7)	0.3 (0.8)	0.01	0.9	56.3	**<0.001**
TMT-A	69.0 (27.4)	86.6 (39.1)	69.8 (24.4)	105.7 (36.5)	0.9	0.4	9.4	**<0.001**
TMT-B	163.1 (74.4)	228.8 (79.4)	188.0 (62.6)	263.7 (70.3)	0.2	0.6	11.8	**<0.001**
SVF	17.0 (3.8)	12.4 (5.4)	16.7 (4.0)	8.6 (5.2)	2.9	0.1	23.4	**<0.001**
CDT	4.1 (0.7)	3.1 (0.6)	4.2 (0.5)	3.4 (0.6)	0.7	0.4	17.5	**<0.001**

ǂ and ǂ Represent the significant difference between YHC and OHC, as well as EOAD and LOAD ($p<0.05$), respectively. Interactive effects comprise the factors of onset age (<65 or ≥65 years) and disease status (controls or patients). Abbreviations: YHC, young healthy controls; EOAD, early-onset Alzheimer's disease; OHC, old healthy controls; LOAD, late-onset Alzheimer's disease; CDR, Clinical Dementia Rating; MMSE, Mini-Mental State Examination; GDS, Geriatric Depression Scale; LM, Logical Memory; TMT-A/B, Trail Making Test, part A/B; SVF, Semantic Verbal Fluency.

Supplementary Materials 3

Effects of white matter hyperintensities on fixel-based analysis

Increasing evidence shows that AD is a multifactorial and heterogeneous disease with multiple contributors to its pathophysiology, including cerebrovascular disease [9]. Among them, WMH is the typical imaging marker of cerebral small vascular disease (CSVD) [10]. We thus calculated WMH through semi-quantitative visual assessment [11]. We found that the elderly group (LOAD and LONC) had more WMH burden than the young group (EONC and EOAD); while dementia group (EOAD and LOAD) had more WMH burden than the healthy group (EONC and LONC).

Supplementary Table 3. The distribution of WMH burden among four groups in two databases.

ZJU database (n, %)	WMH Fazekas score (0, 1, 2, 3)
EOAD	9 (29.0), 17 (54.8), 3 (9.7), 2 (6.5)
EONC	26 (40.6), 35 (54.7), 2 (3.13), 1 (1.6)
LOAD	2 (4.4), 17 (37.8), 10 (22.2), 16 (35.6)
LONC	11 (23.9), 17 (37.0), 7 (15.2), 11 (23.9)
ADNI database (n, %)	WMH Fazekas score (0, 1, 2, 3)
EOAD	12 (70.6), 4 (23.5), 1 (5.8), 0 (0)
EONC	14 (45.2), 13 (41.9), 2 (6.5), 2 (6.5)
LOAD	10 (33.3), 4 (13.3), 11 (36.7), 5 (16.7)
LONC	17 (50.0), 10 (29.4), 6 (17.6), 1 (2.9)

Considering that many difference regions in FBA results partially overlapped with paraventricular WMH, we further re-performed FBA analysis with WMH as a covariable. After adjustment for WMH, our results show that the trend in FBA outcomes remained mostly unchanged in both the databases of ZJU and ADNI, but the range of differences between groups became smaller. Basically, consistent with recent findings, our results suggest that WMH does contribute to the microstructural lesions in AD patients to some extent [12]. Thus, it is necessary to take CSVD into account in future AD studies.

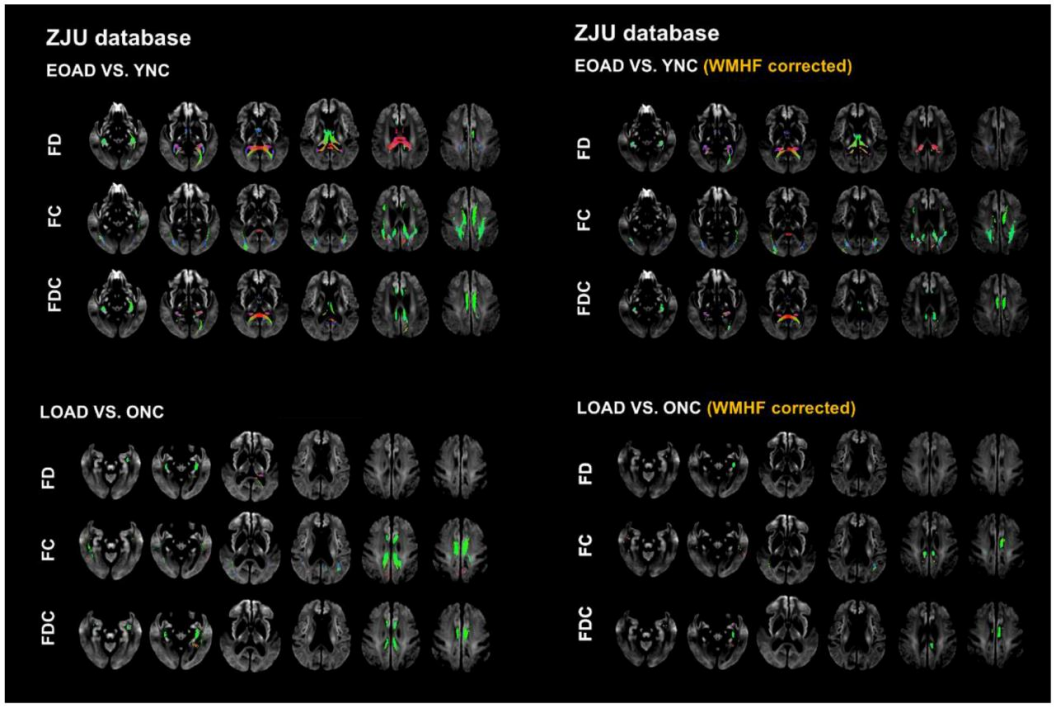

Supplementary Figure 2. The location reference and fiber tract-specific reduction in EOAD/LOAD versus controls (ZJU database) from whole-brain fixel-based analysis, results corrected by Fazekas WMH score. We color-coded the significant streamlines by the effect size expressed as a percentage relative to the control groups. Abbreviations: ZJU, Zhejiang University; FD, fiber density; FC, fiber bundle cross-section; FDC, fiber density and bundle cross-section.

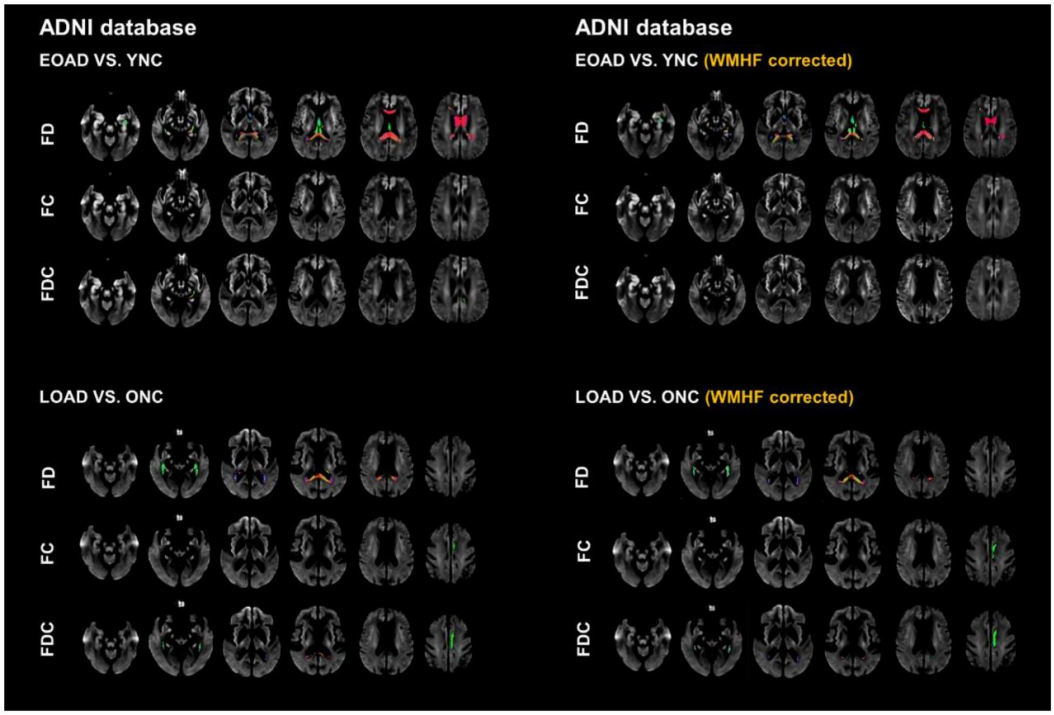

Supplementary Figure 3. The location reference and fiber tract-specific reduction in EOAD/LOAD versus controls (ADNI database) from whole-brain fixel-based analysis, results corrected by Fazekas WMH score. We color-coded the significant streamlines by the effect size expressed as a percentage relative to the control groups. Abbreviations: ADNI, Alzheimer's Disease Neuroimaging Initiative; FD, fiber density; FC, fiber bundle cross-section; FDC, fiber density and bundle cross-section.

Supplementary Materials 4

Association between fixel-based analysis metrics and cognitive/PET data across groups

Across four groups (EOAD, YHC, LOAD, and OHC), we correlated both the mean FD and FC of significant tracts in group differences analyses with the cognitive score (uncorrected, $p < 0.001$, controlling age and gender). Additionally, in the ADNI database, we also correlated both the mean FD and FC of significant tracts in group differences analyses with the PET data (uncorrected, $p < 0.001$, controlling age and gender).

ZJU database

Regarding the WM microstructural metric, we found that MMSE was related with FD in left PTR (r = 0.23); CDT was related with FD in the bilateral PTR (r = 0.26 and 0.24, respectively); delay recall was related with FD in the left ventral cingulum (r = 0.27); SVF was related with FD in the left ventral cingulum (r = 0.26) and left ILF/IFOF (r = 0.25); TMT-A was related with FD in the SCC (r = -0.24), bilateral dorsal cingulum (r = -0.24/-0.23, respectively), and left ventral cingulum (r = -0.27); TMT-B was related with FD in the ventral cingulum (r = -0.23). Regarding the macrostructural metric, we found that MMSE was related with FC in the dorsal cingulum (r = 0.24), delay recall was related with FC in the fornix column and body (r = -0.29), bilateral fornix HP (r = -0.25/-0.25, respectively); while TMT-B was related with FC in the right PTR (r = -0.23).

Within EOAD patients, we found that TMT-A was related with the left dorsal cingulum (r = -0.59); TMT-B was related with SCC (r = -0.57) and left dorsal cingulum (r = -0.57). Bycontrast, within LOAD patients, we found that SVF was related to left ventral cingulum (r = 0.41).

ADNI database

Regarding the WM microstructural metric, we found that MMSE was related with FD in the SCC (r = 0.38), fornix column and body (r = 0.40), left PTR (r = 0.35); CDR was related with FD in the SCC (r = -0.31), fornix column and body (r = -0.36), right dorsal cingulum (r = -0.31), left ILF/IFOL (r = -0.35); SVF was related with FD in the SCC (r = 0.37), fornix column and body (r = 0.46), and bilateral PRT (r = 0.29/0.49, respectively); TMT-B was related with FD in the SCC (r = -0.31) and fornix column and body (r = -0.41), left PRT (r = -0.32). Regarding the WM macrostructural metric, we found that MMSE was related with FC in the fornix column and body (r = -0.37), SVF was related with FC in the left dorsal cingulum (r = 0.35), TMT-A was related with FC in the SCC (r = -0.36), bilateral dorsal cingulum (r = -0.35/-0.48, respectively), and left PTR (r = -0.33); TMT-B was related with FC in the SCC (r = -0.37). Further, we found mean tau retention of Braak I-II was related with FC in the right PTR (r = 0.83).

Within EOAD patients, we found that IST was related with the fornix column and body (r=0.71). Bycontrast, within LOAD patients, we found that SVF was related with the left PTR (r=0.55), SCC (r=0.49), right dorsal cingulum (r=0.52), and left dorsal cingulum (r=0.62); TMT B was related with SCC (r=-0.49), left (r=-0.54) and right (r=-0.56) PTR.

Supplementary Materials 5

Braak ROIs defined by Freesurfer [13]

Braak I-II: bilateral entorhinal and hippocampus

Braak III-IV: bilateral parahippocampal gyrus, fusiform, lingual, amygdala, middle temporal, thalamus, caudantcing, rostantcing, postcing, isthmuscing, insula, inferior temporal, temporal pole.

Braak V-VI: bilateral superior frontal, lateral orbitofrontal, medial orbitofrontal, frontal pole, caudal middle frontal, rostral middle frontal, pars opercularis, pars orbitalis, pars triangularis, lateral occipital, parietal supramarginal, parietal inferior, superior temporal, parietal superior, precuneus, bank superior temporal sulcus, accumbens, tranvtemp, pericalcarine, postcentral, cuneus, precentral, paracentral.

More detailed information are available in https://adni.bitbucket.io/reference/docs/UCBERKELEYAV1451/UCBERKELEYAV1451_Methods_20171114.pdf

Supplementary References

1. Li KC, Luo X, Zeng QZ, Xu XJ, Huang PY, Shen ZJ, Xu JJ, Zhou J, Zhang MM. Distinct patterns of interhemispheric connectivity in patients with early- and late-onset Alzheimer's disease. Front Aging Neurosci. 2018; 10:261. https://doi.org/10.3389/fnagi.2018.00261 PMID:30237764

2. Folstein MF, Robins LN, Helzer JE. The mini-mental state examination. Arch Gen Psychiatry. 1983; 40:812.

https://doi.org/10.1001/archpsyc.1983.01790060110016
PMID:6860082

3. Morris JC. The clinical dementia rating (CDR): current version and scoring rules. Neurology. 1993; 43:2412–14. https://doi.org/10.1212/wnl.43.11.2412-a PMID:8232972

4. Sheikh JI, Yesavage JA. Geriatric Depression Scale (GDS): recent evidence and development of a shorter version. Clinical Gerontologist: The Journal of Aging and Mental Health. 1986. https://doi.org/10.1300/J018v05n01_09

5. Dubois B, Feldman HH, Jacova C, Dekosky ST, Barberger-Gateau P, Cummings J, Delacourte A, Galasko D, Gauthier S, Jicha G, Meguro K, O'brien J, Pasquier F, et al. Research criteria for the diagnosis of Alzheimer's disease: revising the NINCDS-ADRDA criteria. Lancet Neurol. 2007; 6:734–46. https://doi.org/10.1016/S1474-4422(07)70178-3 PMID:17616482

6. Canu E, Agosta F, Spinelli EG, Magnani G, Marcone A, Scola E, Falautano M, Comi G, Falini A, Filippi M. White matter microstructural damage in Alzheimer's disease at different ages of onset. Neurobiol Aging. 2013; 34:2331–40. https://doi.org/10.1016/j.neurobiolaging.2013.03.026 PMID:23623599

7. Cho H, Choi JY, Lee SH, Lee JH, Choi YC, Ryu YH, Lee MS, Lyoo CH. Excessive tau accumulation in the parieto-occipital cortex characterizes early-onset Alzheimer's disease. Neurobiol Aging. 2017; 53: 103–11. https://doi.org/10.1016/j.neurobiolaging.2017.01.024 PMID:28254589

8. Nichols TE, Holmes AP. Nonparametric permutation tests for functional neuroimaging: a primer with examples. Hum Brain Mapp. 2002; 15:1–25. https://doi.org/10.1002/hbm.1058 PMID:11747097

9. Sweeney MD, Montagne A, Sagare AP, Nation DA, Schneider LS, Chui HC, Harrington MG, Pa J, Law M, Wang DJJ, Jacobs RE, Doubal FN, Ramirez J, et al. Vascular dysfunction-The disregarded partner of Alzheimer's disease. Alzheimers Dement. 2019; 15:158–167. https://doi.org/10.1016/j.jalz.2018.07.222 PMID:30642436

10. Wardlaw JM, Smith C, Dichgans M. Small vessel disease: mechanisms and clinical implications. Lancet Neurol. 2019; 18:684–96. https://doi.org/10.1016/S1474-4422(19)30079-1 PMID:31097385

11. Fazekas F, Chawluk JB, Alavi A, Hurtig HI, Zimmerman RA. MR signal abnormalities at 1.5 T in Alzheimer's dementia and normal aging. AJR Am J Roentgenol. 1987; 149:351–6. https://doi.org/10.2214/ajr.149.2.351 PMID:3496763

12. Finsterwalder S, Vlegels N, Gesierich B, Araque Caballero MÁ, Weaver NA, Franzmeier N, Georgakis MK, Konieczny MJ, Koek HL, and Dominantly Inherited Alzheimer Network (DIAN), Karch CM, Graff-Radford NR, Salloway S, Oh H, et al. Small vessel disease more than Alzheimer's disease determines diffusion MRI alterations in memory clinic patients. Alzheimers Dement. 2020; 16:1504–14. https://doi.org/10.1002/alz.12150 PMID:32808747

13. Fischl B. FreeSurfer. Neuroimage. 2012; 62:774–81. https://doi.org/10.1016/j.neuroimage.2012.01.021 PMID:22248573